Effects of dissipation on disordered quantum spin models

L. F. Cugliandolo,[1,2] D. R. Grempel,[3] G. Lozano,[4,5] and H. Lozza[5]
[1]*Laboratoire de Physique Théorique de l'École Normale Supérieure, 24 rue Lhomond, 75231 Paris Cedex 05, France*
[2]*Laboratoire de Physique Théorique et Hautes Énergies, Jussieu, 1er étage, Tour 16, 4 Place Jussieu, 75252 Paris Cedex 05, France*
[3]*CEA-Saclay, DSM/DRECAM/SPCSI, 91191 Gif-sur-Yvette Cedex, France*
[4]*Department of Mathematics, Imperial College London, 180 Queen's Gate, London SW7 2BZ, United Kingdom*
[5]*Departamento de Física, FCEyN, Universidad de Buenos Aires, Pabellón I, Ciudad Universitaria, 1428 Buenos Aires, Argentina*
(Received 10 February 2004; revised manuscript received 10 May 2004; published 30 July 2004)

We study the effects of the coupling to an Ohmic quantum environment on the static and dynamical properties of a class of disordered spin models in a transverse magnetic field using a method of direct spin summation. We discuss the influence of the environment on various features of the phase diagram of the models as well as on the stability of the possible phases.

DOI: 10.1103/PhysRevB.70.024422 PACS number(s): 75.10.Jm, 75.10.Nr, 75.40.Gb

I. INTRODUCTION

The coupling of quantum two-level systems (TLS) to a dissipative environment has decisive effects on their dynamical properties. The case of dilute systems, in which interactions between the TLS can be neglected, has been extensively investigated in the literature[1,2] and is now well understood. The physics that emerges in the cases in which interactions between the TLS may not be neglected is much less understood.

In this paper we study the effects of a dissipative environment on the equilibrium and dynamical properties of quantum *glassy* systems. Spin-glass phases in which quantum fluctuations play an important role were found in a number of experimental systems[3–5] and the importance of interactions on the properties of tunneling defects in structural glasses was recently demonstrated.[6]

Mean-field[7] and finite dimensional[8] quantum spin-glass models have been studied intensively in the last few years. The effects of a coupling to the environment have been discussed for some of these models such as the quantum spherical p-spin glass model,[9–11] the $SU(N)$ random Heisenberg model in the limit $N\to\infty$,[12] and the quantum random walk problem.[13] In all these cases the relevant degrees of freedom are continuous, a fact that makes analytical treatments possible.

Here we analyze the more realistic case of systems of interacting $S=1/2$ spins coupled to a bath of harmonic oscillators. We consider the case in which the interactions involve p-uplets of spins and are of infinite range. For $p=2$ we recover a model for metallic spin glasses studied previously.[14] For $p>3$ the model exhibits richer behavior,[15–18] including the possibility of having first order transition lines.

We use a method of direct spin summation (DSS) first used in the context of disordered spin models by Goldschmidt and Lai.[19] In this method the disorder-averaged free-energy density is computed using the replica method to average over the random quenched interactions. Next, a Trotter decomposition is performed in order to express the partition function of the resulting single-site self-consistent problem as a sum over different contributions, each coming from a possible spin history $\sigma(\tau)=\pm 1$. The continuous imaginary-time variable $0\leqslant\tau\leqslant\beta\hbar$ is discretized on a grid $\tau_t=t\beta\hbar/M$, $t=0,\cdots,M-1$, and the partition function is computed by numerically performing the *exact* sum over the 2^M possible discrete spin histories, $\sigma_t\equiv\sigma(\tau_t)=\pm 1$. Physical results are obtained repeating this procedure for various values of M and extrapolating to $M\to\infty$.

The main conclusion of this work is that the coupling to the enviromement reduces the strength of the quantum fluctuations thus favoring the appearance of the spin-glass phase. Whereas for $p=2$ the phase transition is always second order, for $p\geqslant 3$ quantum fluctuations drive the transition first order below a tricritical temperature $T^\star$. We find that $T^\star$ decreases with the strength of the coupling to the bath. For $p\geqslant 3$ a dynamic transition precedes the equilibrium phase transition. The coupling to the bath also stabilizes the dynamic glassy phase.

The organization of the paper is as follows. In Sec. II we introduce the coupled p-spin-bath model and the formalism that we use to solve it. In Sec. III we discuss the numerical method and present our results. Section IV contains our conclusions.

II. THE MODEL

We are interested in disordered Ising spin models in a transverse field described by Hamiltonians of the type

$$H_s = H_L - \Gamma\sum_{i=1}^{N}\hat{\sigma}_i^x \tag{1}$$

with

$$H_L = -\sum_{i_1<\cdots<i_p}^{N} J_{i_1,\ldots,i_p}\hat{\sigma}_{i_1}^z\cdots\hat{\sigma}_{i_p}^z. \tag{2}$$

Here, $\hat{\sigma}^x$, $\hat{\sigma}^y$, $\hat{\sigma}^z$ are the standard Pauli matrices, $J_{i_1\cdots i_p}$ denotes a quenched random exchange between groups of p spins, Γ is a transverse magnetic field, and N is the total number of spins. The sum runs over all possible p-uplets of spins. The model is then fully connected and mean-field in

character. The transverse field introduces quantum fluctuations in what would otherwise be a purely classical model.

To completely define the model we must choose p and the distribution $\mathcal{P}[J]$ of random interactions. We consider the case in which the random independent variables $J_{i_1,\ldots,i_p}$ are Gaussian with zero mean and variance $p!J^2/2N^{p-1}$. The scaling of the variance with N is chosen so as to ensure a good thermodynamic limit.

We study the thermodynamics and some aspects of the nonequilibrium dynamics of model 1 coupled to a quantum environment represented by a set of $\tilde{N}$ independent harmonic oscillators. We assume that the oscillators are in thermal equilibrium and that each of the spins in the system is coupled to a different subset of these.

The bosonic Hamiltonian of the isolated reservoir is

$$H_b = \sum_{l=1}^{\tilde{N}} \frac{1}{2m_l}\hat{p}_l^2 + \sum_{l=1}^{\tilde{N}} \frac{1}{2} m_l \omega_l^2 \hat{x}_l^2. \tag{3}$$

The coordinates $\hat{x}_l$ and the momenta $\hat{p}_l$ satisfy canonical commutation relations. For simplicity we consider a bilinear coupling

$$H_{sb} = -\sum_{i=1}^{N} \hat{\sigma}_i^z \sum_{l=1}^{\tilde{N}} c_{il}\hat{x}_l \tag{4}$$

that involves only the oscillator coordinates. The Hamiltonian for the coupled system is then given by

$$H = H_s + H_b + H_{sb} + H_{ct}, \tag{5}$$

where we added a counter term

$$H_{ct} = \sum_{l=1}^{\tilde{N}} \frac{1}{2m_l\omega_l^2}\left(\sum_{i=1}^{N} c_{il}\hat{\sigma}_i^z\right)^2, \tag{6}$$

whose effect is to eliminate a possible mass normalization induced by the coupling to the bath.[2]

The partition function of the combined system for a particular realization of the bonds

$$Z = \mathrm{Tr}[e^{-\beta H}] \tag{7}$$

involves a sum over all states of the system and of the bath. The trace over the variables of the bath can be performed explicitly using standard techniques.[2,20,21] The result of tracing out these variables can be expressed in terms of the spectral function of the bath

$$I_{ij}(\omega) \equiv \frac{\pi}{2}\sum_{l=1}^{\tilde{N}} \frac{c_{il}c_{jl}}{m_l\omega_l}\delta(\omega-\omega_l) = \delta_{ij} I(\omega). \tag{8}$$

We chose to study the effect of an Ohmic bath parameterized as

$$I(\omega) = 2\eta\hbar\omega\Theta(\omega_{\max}-\omega) \tag{9}$$

with η the friction constant, $\omega_{\max}$ an ultraviolet cutoff and $\Theta(x)$ the Heaviside theta function.

This problem can be mapped onto a *classical* Ising model using the Totter-Suzuki formalism.[15,19,22] This amounts to writing the path integral for the partition function as a sum over spin and oscillator variables evaluated on a discrete imaginary-time grid on the points $\tau_t = \beta\hbar/Mt$ labeled by the index $t=0,\ldots,M-1$. Periodic boundary conditions are imposed on the discretized time axis. To recover the correct representation of the trace the limit $M\to\infty$ should be ultimately taken. The finite M expression yields a sequence of M approximants to the asymptotic $M\to\infty$ formula.

The Mth approximant of the "reduced" partition function obtained after integrating out the bath is

$$Z = \mathrm{Tr}_{\{\sigma_i^t\}}\exp\left\{\frac{\beta}{M}\sum_{t=0}^{M-1}\sum_{i_1<\cdots<i_p}^{N} J_{i_1\cdots i_p}\sigma_{i_1}^t\cdots\sigma_{i_p}^t + \sum_{t=0}^{M-1}\sum_{i=1}^{N}[A + B\sigma_i^t\sigma_i^{(t+1)}] - \sum_{t,t'=0}^{M-1}\sum_{i=1}^{N}(1-\sigma_i^t\sigma_i^{t'})C_{(t-t')}\right\}, \tag{10}$$

where

$$A = \frac{1}{2}\ln\left[\sinh\left(\frac{\beta\Gamma}{M}\right)\cosh\left(\frac{\beta\Gamma}{M}\right)\right], \tag{11}$$

$$B = \frac{1}{2}\ln\left[\coth\left(\frac{\beta\Gamma}{M}\right)\right], \tag{12}$$

$$C_{(t-t')} = \frac{2\eta}{\pi\hbar}\int_0^{\omega_{\max}} d\omega \times \frac{\cosh[\omega\beta\hbar((t-t')/M-1/2)]\sinh^2(\omega\beta\hbar/2M)}{\omega\sinh(\omega\beta\hbar/2)}. \tag{13}$$

The trace represents the sum over all $2^{N\times M}$ distinct classical Ising spin configurations, $\sigma_i^t = \pm 1$, for each spin, $i=1,\ldots,N$, evaluated at each time-slice, $t=0,\ldots,M-1$.

The disordered averaged free-energy is calculated using the replica trick[23]

$$\beta\overline{F} = -\overline{\ln Z} = -\lim_{n\to 0}\frac{\overline{Z^n}-1}{n}. \tag{14}$$

After some standard manipulations, and up to some irrelevant factors, we obtain

$$\overline{Z^n} = \prod_{a,b=1}^{n}\prod_{t,t'=0}^{M-1}\int \mathcal{D}Q^{atbt'}\mathcal{D}\Lambda^{atbt'}\exp[-NP(\Lambda,Q)], \tag{15}$$

with

$$P(\Lambda,Q)=\sum_{a,b=1}^{n}\sum_{t,t'=0}^{M-1}\left[\frac{\Lambda^{atbt'}}{M^2}Q^{atbt'}-\frac{\beta^2J^2}{4M^2}(Q^{atbt'})^{\bullet p}+\mathcal{C}_{(t-t')}\delta^{ab}(1-Q^{atbt'})\right]-\ln\mathrm{Tr}_{\{\sigma^{at}\}}e^{H_{\mathrm{eff}}},\quad(16)$$

$$H_{\mathrm{eff}}=\sum_{a,b=1}^{n}\sum_{t,t'=0}^{M-1}\frac{\Lambda^{atbt'}}{M^2}\sigma^{at}\sigma^{bt'}+\sum_{a=1}^{n}\sum_{t=0}^{M-1}\left[A+B\sigma^{at}\sigma^{a(t+1)}\right],\quad(17)$$

where the bullet is used to distinguish the ordinary power from the matrix power. In the thermodynamic limit, $N\to\infty$, the integrals in $\overline{Z^n}$ can be evaluated with the saddle point method at the expense of interchanging the order of the $N\to\infty$ and $n\to0$ limits. The disordered-averaged free-energy per spin is then

$$\beta\overline{f}=\lim_{n\to0}\frac{P[\Lambda_0,Q_0]}{n},\quad(18)$$

where Λ_0 and Q_0 satisfy

$$\left.\frac{\delta P(Q,\Lambda)}{\delta Q}\right|_{Q_0,\Lambda_0}=0,\qquad\left.\frac{\delta P(Q,\Lambda)}{\delta\Lambda}\right|_{Q_0,\Lambda_0}=0.\quad(19)$$

Hereafter we omit subscripts in the saddle-point values Q_0 and Λ_0. The disorder-averaged entropy per spin is easily obtained from the disorder-averaged free-energy density and

$$-\frac{\overline{s}}{k_B}=\beta\overline{f}+\frac{1}{n}\sum_{a,b=1}^{n}\sum_{t,t'=0}^{M-1}\left[\frac{\beta^2J^2}{2M^2}(Q^{atbt'})^{\bullet p}-\delta^{ab}(1-Q^{atbt'})\frac{\partial\mathcal{C}_{(t-t')}}{\partial\beta}\right]+\frac{\beta\Gamma}{\sinh(2\beta\Gamma/M)}\left[\cosh(2\beta\Gamma/M)-\frac{1}{n}\sum_{a=1}^{n}Q^{a(t+1)at}\right].\quad(20)$$

Another physical observable of interest is the magnetic susceptibility

$$\chi=\left.\frac{\partial\mathcal{M}}{\partial h}\right|_{h=0},\quad(21)$$

where $\mathcal{M}=N^{-1}\Sigma_{i=1}^{N}\overline{\langle\sigma_i^z\rangle}$ is the total disorder-averaged magnetization and h a longitudinal external magnetic field. In terms of $Q^{atbt'}$ the susceptibility is given by

$$\chi=\frac{\beta}{M^2}\sum_{a,b=1}^{n}\sum_{t,t'=0}^{M-1}Q^{atbt'}.\quad(22)$$

The right-hand sides of Eqs. (20) and (22) should be evaluated at the saddle point.

The matrix elements $Q^{atbt'}$ are the order parameters of the model

$$Q^{atbt'}=\frac{1}{N}\sum_{i=1}\overline{\langle\sigma_i^{at}\sigma_i^{bt'}\rangle}.\quad(23)$$

Because of the translational invariance in the Trotter time direction the diagonal terms in the replica indices depend on the time difference only

$$Q^{atat'}=q_d(t-t').\quad(24)$$

Notice that due to the periodic boundary condition $q_d(t)=q_d(M-t)$. In addition, as $q_d(0)=1$, only $(t-t')=1,2,\cdots,\mathrm{int}M/2$ need to be considered. The off-diagonal elements in the replica indices, $Q^{atbt'}$ with $a\neq b$, are t and t' independent as shown by Bray and Moore.[24]

In order to determine the different phases of the model, we consider the following *Ansätze*.

(1) *Paramagnetic phase*. The matrices Q and Λ are taken to be diagonal in replica space

$$Q^{atbt'}=q_d(t-t')\delta^{ab},\quad\Lambda^{atbt'}=\lambda_d(t-t')\delta^{ab}.\quad(25)$$

Using Eqs. (16)–(18) the disorder-averaged free-energy per spin can be expressed as

$$\beta\overline{f}=\frac{\beta^2J^2}{4M^2}(p-1)\sum_{t\neq t'}^{M-1}q_d^p(t-t')-\frac{\beta^2J^2}{4M}+\sum_{t\neq t'}^{M-1}\mathcal{C}_{(t-t')}-\ln\mathrm{Tr}_{\{\sigma^t\}}e^{H_{\mathrm{eff}}^{pm}}\quad(26)$$

with

$$H_{\mathrm{eff}}^{pm}=\frac{1}{M^2}\sum_{t\neq t'}^{M-1}\lambda_d(t-t')\sigma^t\sigma^{t'}+\sum_{t=0}^{M-1}\left[A+B\sigma^t\sigma^{(t+1)}\right].\quad(27)$$

Here, $q_d(t-t')$ and $\lambda_d(t-t')$ are obtained self-consistently from the extremum condition by summing over all 2^M spin configurations $\sigma^t=\pm1$:

$$q_d(t-t')=\frac{\mathrm{Tr}_{\{\sigma^t\}}\left[e^{H_{\mathrm{eff}}^{pm}}\sigma^t\sigma^{t'}\right]}{\mathrm{Tr}_{\{\sigma^t\}}e^{H_{\mathrm{eff}}^{pm}}},\quad(28)$$

$$\lambda_d(t-t')=\frac{\beta^2J^2p}{4}q_d^{p-1}(t-t')+M^2\mathcal{C}_{(t-t')}.\quad(29)$$

(2) *Equilibrium spin-glass phase*. In order to characterize this phase we use a one-step replica symmetry breaking (RSB) *Ansatz*

$$Q^{atbt'}=[q_d(t-t')-q_{\mathrm{ea}}]\delta^{ab}+q_{\mathrm{ea}}\epsilon^{ab},\quad(30)$$

$$\Lambda^{atbt'}=[\lambda_d(t-t')-\lambda_{\mathrm{ea}}]\delta^{ab}+\lambda_{\mathrm{ea}}\epsilon^{ab},\quad(31)$$

where ϵ^{ab} is a block-diagonal matrix in replica space

$$\epsilon^{ab}=\begin{cases}1 & \text{if } a \text{ and } b \text{ belong to the same } m\times m\\ & \text{diagonal block,}\\ 0 & \text{otherwise.}\end{cases}\quad(32)$$

The parameter m will be referred below as the *breakpoint*.

Using Eqs. (16)–(18) the disordered-averaged free-energy density becomes

$$\beta\overline{f} = \frac{\beta^2 J^2}{4M^2}(p-1)\sum_{t\neq t'}^{M-1} q_d^p(t-t') + (m-1)\frac{\beta^2 J^2}{4}(p-1)q_{\rm ea}^p$$

$$-\frac{\beta^2 J^2}{4M} - \frac{1}{m}\ln\int d\chi(\mathrm{Tr}_{\{\sigma^t\}} e^{H_{\rm eff}^{\rm esg}})^m + \sum_{t\neq t'}^{M-1} \mathcal{C}_{(t-t')} \qquad (33)$$

with

$$H_{\rm eff}^{\rm esg} = \frac{1}{M^2}\sum_{t\neq t'}^{M-1}(\lambda_d(t-t') - \lambda_{\rm ea})\sigma^t\sigma^{t'} - \frac{\lambda_{\rm ea}}{M} + \frac{\sqrt{2\lambda_{\rm ea}}}{M}x\sum_t^{M-1}\sigma^t$$

$$+\sum_t^{M-1}\left[A + B\sigma^t\sigma^{(t+1)}\right] \qquad (34)$$

and the integration measure

$$d\chi \equiv \frac{dx}{\sqrt{2\pi}} e^{-x^2/2}. \qquad (35)$$

Here and in what follows all integrals over x extend from $-\infty$ to ∞.

As in the paramagnetic phase, the order parameters $q_d(t-t')$, $q_{\rm ea}$, $\lambda_d(t-t')$ and $\lambda_{\rm ea}$ are determined self-consistently from the extremum conditions that involve a sum over all 2^M spin configurations, $\sigma^t = \pm 1$:

$$q_d(t-t') = \frac{\int d\chi\,(\mathrm{Tr}_{\{\sigma^t\}} e^{H_{\rm eff}^{\rm esg}})^{m-1}(\mathrm{Tr}_{\{\sigma^t\}} e^{H_{\rm eff}^{\rm esg}}\sigma^t\sigma^{t'})}{\int d\chi\,(\mathrm{Tr}_{\{\sigma^t\}} e^{H_{\rm eff}^{\rm esg}})^m}, \qquad (36)$$

$$q_{\rm ea} = \frac{\int d\chi\,(\mathrm{Tr}_{\{\sigma^t\}} e^{H_{\rm eff}^{\rm esg}})^{m-2}(\mathrm{Tr}_{\{\sigma^t\}} e^{H_{\rm eff}^{\rm esg}}\sum_t \sigma^t/M)^2}{\int d\chi\,(\mathrm{Tr}_{\{\sigma^t\}} e^{H_{\rm eff}^{\rm esg}})^m}, \qquad (37)$$

$$\lambda_d(t-t') = \frac{\beta^2 J^2 p}{4} q_d^{p-1}(t-t') + M^2\mathcal{C}_{(t-t')}, \qquad (38)$$

$$\lambda_{\rm ea} = \frac{\beta^2 J^2 p}{4} q_{\rm ea}^{p-1}. \qquad (39)$$

As it has been discussed in a number of papers on classical[25] and quantum[15–17,26] spin-glass models, two choices for the determination of the parameter m lead to physically different results. The use of the extremum condition, that corresponds to taking the value of m at which the disorder-averaged free-energy is stationary, leads to

$$m = \Gamma^{-1}\left[m^2\frac{\beta^2 J^2 p}{4}(p-1)q_{\rm ea}^p + \ln\int d\mathcal{X}\,(\mathrm{Tr}_{\{\sigma^t\}} e^{H_{\rm eff}^{\rm esg}})^m\right], \qquad (40)$$

where

$$I = \frac{\int d\mathcal{X}\,(\mathrm{Tr}_{\{\sigma^t\}} e^{H_{\rm eff}^{\rm esg}})^m \ln(\mathrm{Tr}_{\{\sigma^t\}} e^{H_{\rm eff}^{\rm esg}})}{\int d\mathcal{X}\,(\mathrm{Tr}_{\{\sigma^t\}} e^{H_{\rm eff}^{\rm esg}})^m}. \qquad (41)$$

With this choice one describes the equilibrium properties of the model.

This *Ansatz* yields the exact solution[17] to the spherical version of the $p \geqslant 3$ model. The $p=2$ spherical model is solved by a simpler replica symmetric form.

We do not expect the one-step RSB *Ansatz* to be stable everywhere in the phase diagram in the case of the discrete spin models that we investigate here. The stability of the one-step *Ansatz* for the quantum models can be tested by extending to the quantum case the classical analysis of de Almeida and Thouless.[27] When the lowest eigenvalue of the stability matrix (also called *replicon*) vanishes, the one-step RSB *Ansatz* is marginally stable. When the replicon is negative, this *Ansatz* is unstable.

By evaluation of the replicon for the values of the order parameters and the breakpoint obtained from the extremum conditions we found that the one-step RSB *Ansatz* is unstable in the full spin-glass phase when $p=2$ [Sherrington-Kirkpatrick (SK)] model indicating the need to break the replica symmetry further.

In the case of the $p \geqslant 3$ classical spin model, the one-step RSB *Ansatz* is unstable below a temperature $T_g < T_s$ as shown by Gardner[28] in the classical case. Thus, the solution for the classical Ising p spin model also requires full RSB at very low temperatures. T_g depends on the parameter p and, as expected, it tends to $T_s = J$ when $p \to 2^+$ and it vanishes when $p \to \infty$. We thus expect to find a Gardner line of instability also when quantum fluctuations are taken into account. A careful study of the dependence of this line on Γ and the coupling to the bath requires solving the quantum problem at rather low temperatures. This is done in Sec. III where we compute the location of the Gardner instability line. As seen in Fig. 8, the region where the one-step RSB static *Ansatz* is unstable is quite small. Outside this region the one-step RSB *Ansatz* is exact and can be used to study the properties of the

$p \geqslant 3$ quantum $S=1/2$ model. Elsewhere, and for $p=2$, we shall regard this solution as a suitable approximation to the correct solution.

(3) *Dynamic spin-glass phase*. The *marginality condition* leads to a different equation for m. With this condition one requires that the saddle-point is only marginally stable, i.e., the matrix of quadratic fluctuations has a zero replicon eigenvalue (and one does not impose the condition of extreme on m). It has been checked by comparison to the real time dynamics,[9] that this condition yields the location of the freezing transition of the spherical quantum p-spin model with $p \geqslant 3$ coupled to the oscillator reservoir at the initial time $t=0$.[10] Here we use it as an indication of where such a dynamic transition line should be located for the discrete quantum spin systems.

Adapting the calculation of de Almeida and Thouless[27] to the quantum problem under study we find that the replicon eigenvalue is given by

$$\lambda_R = P - 2Q + R \tag{42}$$

with

$$P = 1 - kq_{\mathrm{ea}}^{p-2}t, \quad Q = -kq_{\mathrm{ea}}^{p-2}u, \quad R = -kq_{\mathrm{ea}}^{p-2}r. \tag{43}$$

The factors r, u, and t are

$$r = \langle \sigma^a \sigma^b \sigma^c \sigma^d \rangle = \frac{\int d\chi (\mathrm{Tr}_{\sigma^t} e^{H_{\mathrm{eff}}^{\mathrm{dsg}}})^{m-4} \left[\mathrm{Tr}_{\sigma^t} e^{H_{\mathrm{eff}}^{\mathrm{dsg}}} \left(\sum_t \sigma^t / M \right) \right]^4}{\int d\chi (\mathrm{Tr}_{\sigma^t} e^{H_{\mathrm{eff}}^{\mathrm{dsg}}})^m}, \tag{44}$$

$$u = \frac{1}{M^2} \sum_{t\tau} \langle \sigma^{at} \sigma^b \sigma^{a\tau} \sigma^d \rangle = \frac{\int d\chi (\mathrm{Tr}_{\sigma^t} e^{H_{\mathrm{eff}}^{\mathrm{dsg}}})^{m-3} \left[\mathrm{Tr}_{\sigma^t} e^{H_{\mathrm{eff}}^{\mathrm{dsg}}} \left(\sum_t \sigma^t / M \right) \right]^2 \mathrm{Tr}_{\sigma^t} e^{H_{\mathrm{eff}}^{\mathrm{dsg}}} \left(\sum_{tt'} \sigma^t \sigma^{t'} / M^2 \right)}{\int d\chi (\mathrm{Tr}_{\sigma^t} e^{H_{\mathrm{eff}}^{\mathrm{dsg}}})^m}, \tag{45}$$

$$t = \frac{1}{M^4} \sum_{tt'\tau\tau'} \langle \sigma^{at} \sigma^{bt'} \sigma^{a\tau} \sigma^{b\tau'} \rangle = \frac{\int d\chi (\mathrm{Tr}_{\sigma^t} e^{H_{\mathrm{eff}}^{\mathrm{dsg}}})^{m-2} \left[\mathrm{Tr}_{\sigma^t} e^{H_{\mathrm{eff}}^{\mathrm{dsg}}} \left(\sum_{tt'} \sigma^t \sigma^{t'} / M^2 \right) \right]^2}{\int d\chi (\mathrm{Tr}_{\sigma^t} e^{H_{\mathrm{eff}}^{\mathrm{dsg}}})^m}. \tag{46}$$

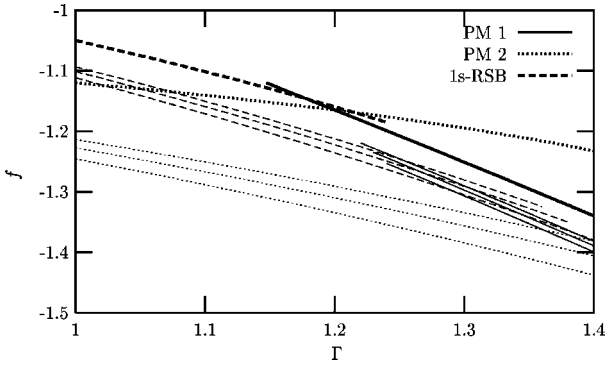

FIG. 1. Disorder-averaged free-energy density, $\overline{f}$, of the quantum $S=1/2$ $p=3$ model at temperature $T=0.3$ as a function of the transverse magnetic field Γ. The coupling to the bath is $\eta=1.0$. The three phases of the model are represented: a physical paramagnet labeled PM1, an unphysical paramagnet that one discard on physical grounds labeled PM2 and the spin glass. The values of $\overline{f}$ obtained for finite M are shown with thin lines [$M=8$ (bottom), $M=9$ (middle), and $M=10$ (top)]. The result of the extrapolation to $M \to \infty$ is displayed with bold lines.

Here, we have defined

$$k \equiv \frac{\beta^2 J^2}{2} p(p-1) \tag{47}$$

and $H_{\mathrm{eff}}^{\mathrm{dsg}}$ is the Hamiltonian of Eq. (34). Finally, the values of $q_d(t-t')$ and q_{ea} are fixed by the extremal conditions.

III. RESULTS

In this section we describe the outcome of solving the equations we derived in the previous section and we discuss how the coupling to the Ohmic bath of harmonic oscillators modifies the behavior of the spin model.

A. Numerical method

The free-energy density and derived magnitudes depend on the parameter M that in practice takes finite values. Several strategies were proposed to study the limit $M \to \infty$. Usadel and Schmitz[29] noted that M should be such that

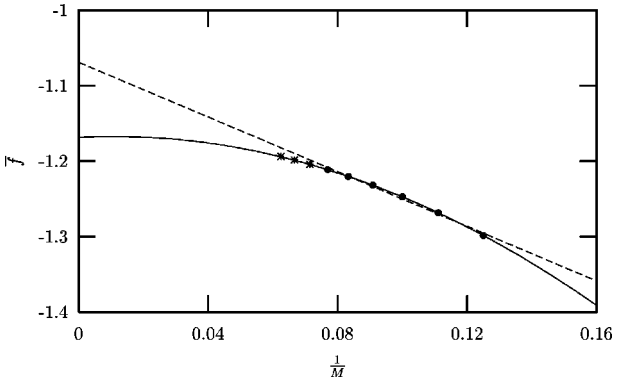

FIG. 2. The critical averaged free-energy density, $\overline{f}$, at inverse temperature $\beta=3.3$, as a function of the inverse number of imaginary-time slices, $1/M$. The coupling to the bath is $\eta=1.0$. The dashed and solid lines are the results of fits linear in $1/M$ and in $1/M^2$, respectively. Circles: results of DSS for $M=8,9,10,11,12$, and 13. Stars: results of DSS for $M=14,15$, and 16.

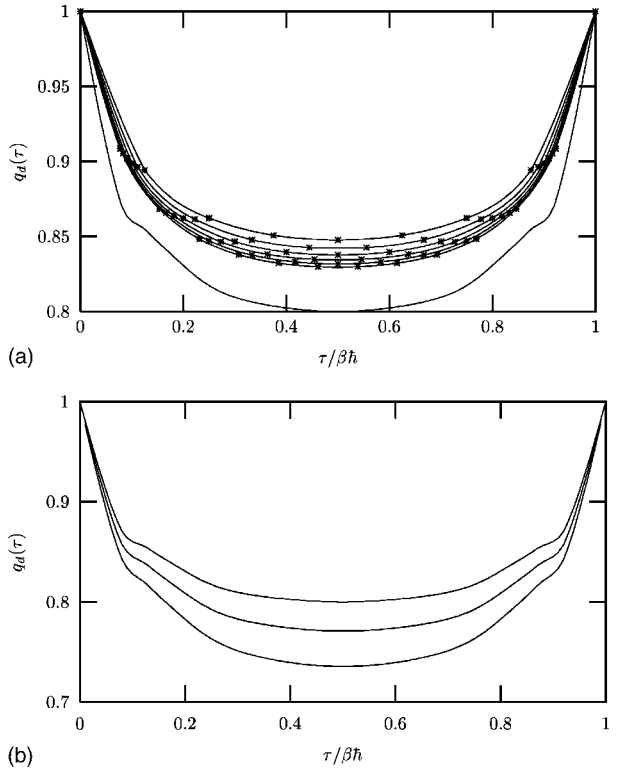

FIG. 3. Upper panel: The diagonal order parameter $q_d(\tau)$ for the $p=3$ model as a function of $\tau/(\beta\hbar)=t/M$ where t is the Trotter index, $t=0,1,\cdots,M$. The temperature is $T=0.3$ and the transverse magnetic field is $\Gamma=0.8$. The coupling to the bath is $\eta=1$. The six upper curves are the solutions for $M=8,9,10,11,12,13$, from top to bottom. The symbols are the actual data and the lines represent the results of the spline interpolation. The lowest curve is the result of the extrapolation to $M\to\infty$. Lower panel: The limiting curve $\lim_{M\to\infty} q_d^M(\tau)$ for three couplings to the environment: $\eta=0$ (bottom curve), $\eta=0.5$ (middle curve), and $\eta=1$ (top curve), The other parameters are the same as in the upper panel. (See text for the details of the method of extrapolation used.)

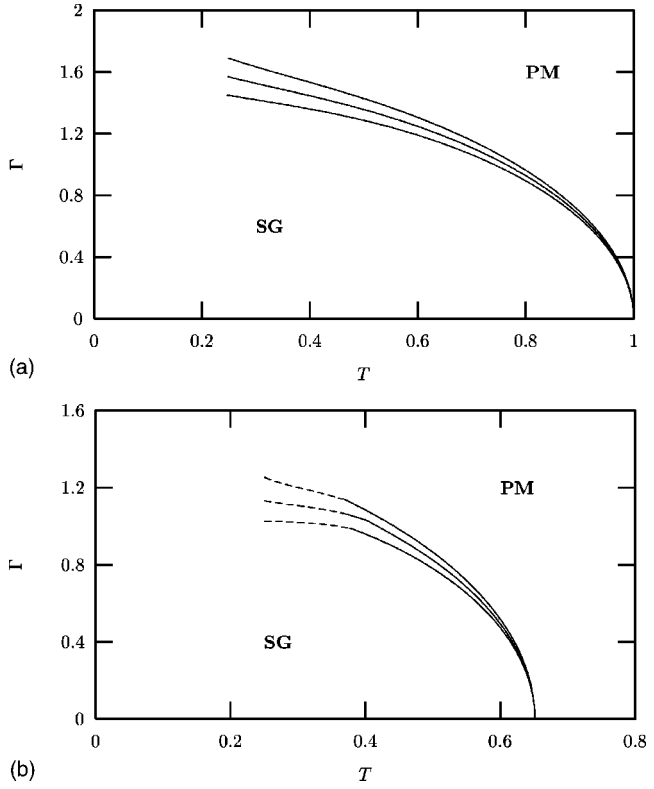

FIG. 4. Upper panel: Static phase diagram for the $p=2$ model as obtained using the DSS technique for finite number of time slices M and extrapolating the data to $M\to\infty$. The three lines correspond to $\eta=0,0.5,1$, from bottom to top. Lower panel: Static phase diagram for the $p=3$ model obtained using the same numerical method. The continuous line (dashed line) indicates a second order (first order) phase transition. The critical lines continue below the lowest value of T for which we trust the algorithm, $T\approx 0.25$, to reach a quantum critical point at $T=0$.

$\beta\Gamma/M\ll 1$. For low temperatures this criterion becomes quickly impractical since one cannot perform the complete sum over states for such large values of M. As an alternative, these authors proposed to use a Monte Carlo procedure to estimate the sum over configurations when M is large.[29,30]

In this paper we adopt another method that has been previously used to study the isolated quantum SK model[19] and $S=1/2$ p-spin models in a transverse field.[15] Physical quantities are computed by DSS for values of M in the range $8\leqslant M\leqslant 13$. The results thus obtained are fitted to series of powers of $1/M$ that allows to perform the extrapolation to $M\to\infty$. In almost all cases the expected[31] $(1/M)^2$ law is verified.

As an example, consider the free-energy density of the different phases of the $p=3$ model with $\eta=1$ (that will be discussed in detail later) displayed in Fig. 1. The four curves correspond to three values of M, $M=8,9,10$, and to the result of the extrapolation to $M\to\infty$, respectively. Figure 2 shows the M dependence of the free energy at the value of the transverse field at which the curves for the paramagnetic and spin-glass phases cross. The circles represent the data for $M=8$, 9, 10, 11, 12, and 13. The dashed and solid lines are the results of fits linear in $1/M$ and in $1/M^2$, respectively.

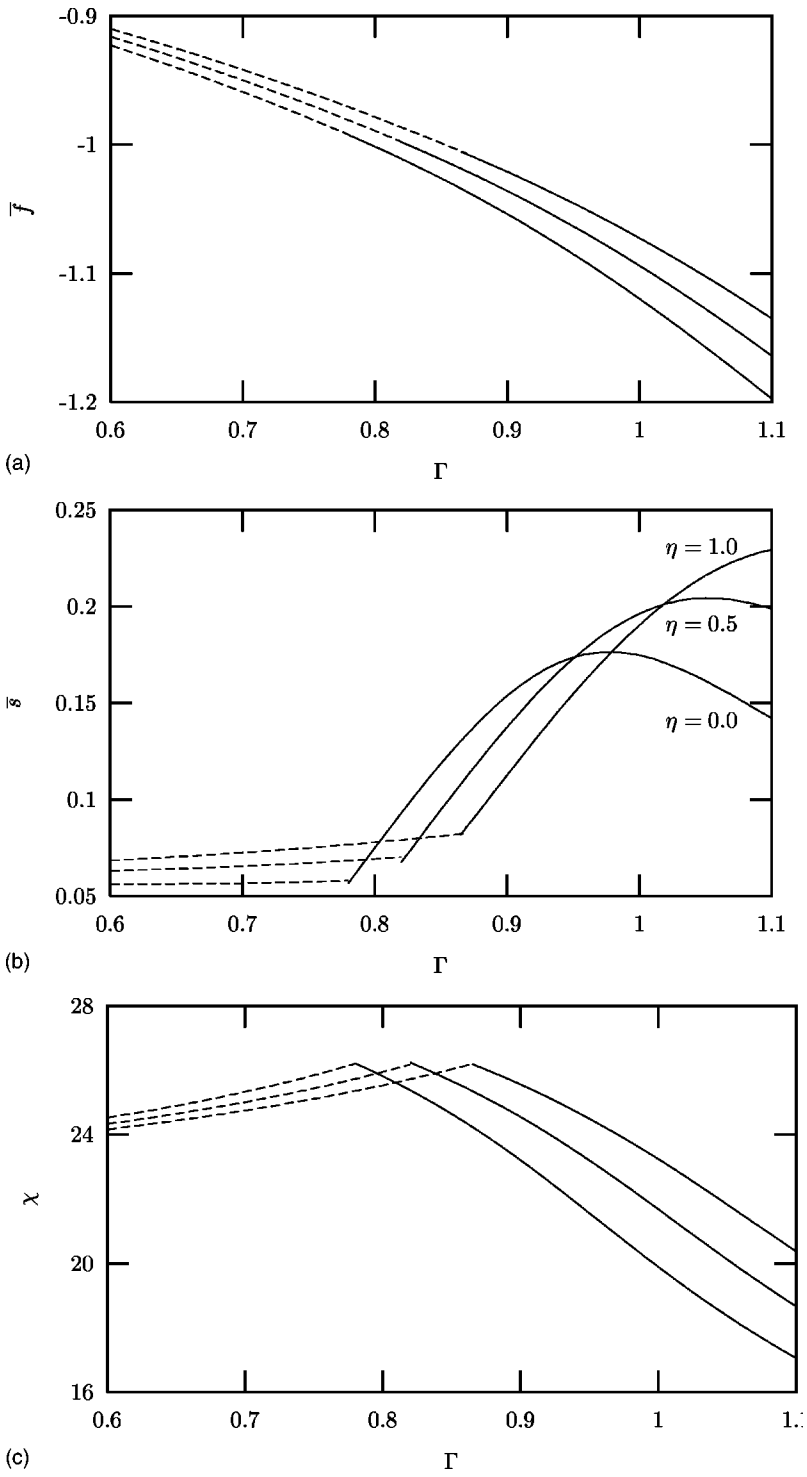

FIG. 5. Free energy density, $\bar{f}$, entropy, $\bar{s}$, and susceptibility, χ, as functions of the transverse field, Γ, for the $p=3$ model at $T=0.5>T_s^*$ for three values of the coupling to the bath, $\eta=0,0.5,1$. The continuous (dashed) line corresponds to the paramagnetic (glassy) phase. The entropy and susceptibility are continuous at the transition indicating a second order phase transition.

The difference between the asymptotic values obtained using these two extrapolations is of the order of 10%. The last three points, represented by stars, are the result of the DSS for $M=14,15,16$. It can be seen that they fall nicely on the $1/M^2$ extrapolation curve obtained for the smaller values of M thus supporting the results of the $1/M^2$ extrapolations that we shall use hereafter.

The same method can be used to determine the diagonal order parameter, $q_d(\tau)$. Since the latter is only known on the imaginary-time grid $0,\beta\hbar/M,2\beta\hbar/M,\cdots,\beta\hbar$ and this depends on M, we first perform a spline interpolation of the data for each value of M and use the interpolated curves as imput for the polynomial extrapolation described earlier.

The method is illustrated in the upper panel of Fig. 3 where we show the diagonal order parameter $q_d(\tau)$ as a function of τ at constant temperature and transverse magnetic field for the $p=3$ model. Data for six values of M, $M=8,\cdots,13$, are represented by the symbols and the lines going through them represent the spline interpolations. The lowest curve is the result of the extrapolation to $M\to\infty$.

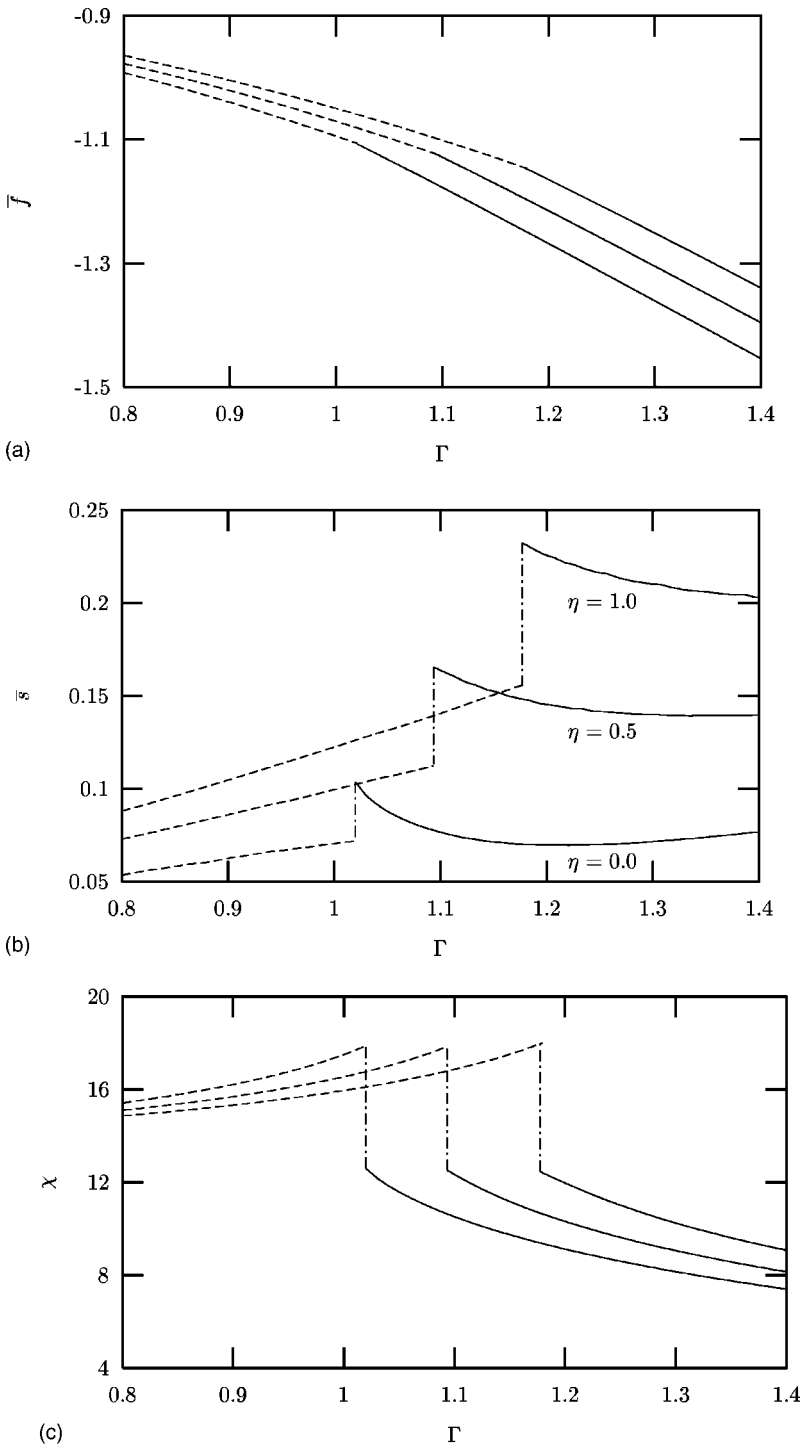

FIG. 6. Free energy, $\overline{f}$, entropy, $\overline{s}$, and susceptibility, χ, as function of the transverse field, Γ, for the $p=3$ model at $T=0.3<T_s^*$ for three values of the coupling to the bath, $\eta=0, 0.5, 1$. The continuous (dashed) line corresponds to the paramagnetic (glassy) phase. The entropy and susceptibility are discontinuous at the transition indicating a first order phase transition.

The method of Goldschmidt and Lai[19] just described is simple to implement and very efficient but it is limited to relatively high temperatures as the extrapolation becomes less and less reliable as the temperature decreases.

B. Static phases

Let us first discuss the effect of the environment on the static phase diagram of the $p=2$ (SK) and $p\geqslant 3$ quantum $S=1/2$ spin models. The spin-glass disorder-averaged free-energy densities are obtained using the one-step RSB *Ansatz* discussed in Sec. II. We discuss the limits of validity of this *Ansatz* later.

As in other disordered quantum spin models[15–17,22] two paramagnetic solutions coexist. As in the spherical p-spin model coupled to a bath the one labeled PM2 in Fig. 1 can be discarded since its entropy becomes negative at sufficiently low temperatures. Thus, we do not discuss it further in this paper.

The critical line (T_s, Γ_s) separating the paramagnetic (PM) and spin-glass (SG) phases is determined by the values of the pairs (T, Γ) where the physical paramagnetic (called PM1 in

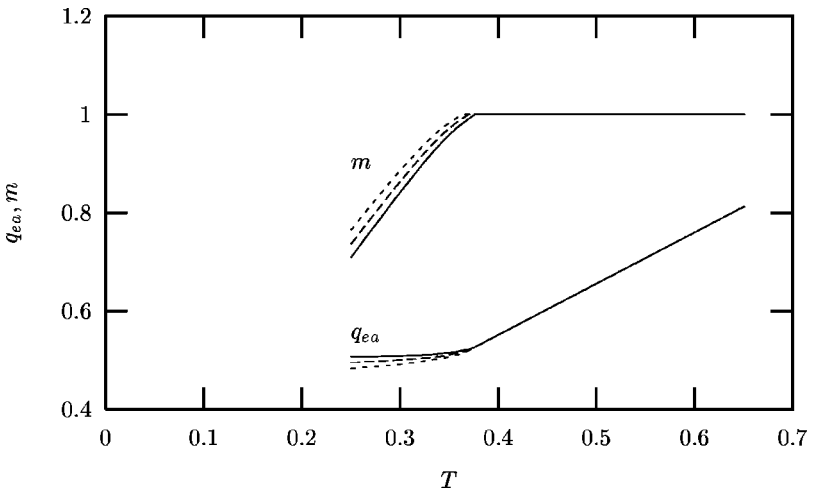

FIG. 7. Dependence of m and q_{ea} on the critical temperature $T_s(\Gamma,\eta)$ for the $p=3$ model. Three values of η are considered, $\eta=0,0.5,1$. For increasing values of η the interval in which $m=1$ increases and, hence, the region where a thermodynamic first order transition occurs decreases.

Fig. 1) and spin-glass free-energy densities cross.

We show in the upper and lower panels of Fig. 4 the static critical line in the (T,Γ) plane separating a high T, high Γ PM from a low T, low Γ SG for the $p=2$ and $p=3$ models, respectively. The three curves in each figure correspond to ($\eta=0$) and two nonzero couplings ($\eta=0.5,1$) from bottom to top.

For both models, the classical transition temperature, T_s^{class}, corresponding to $\Gamma_s\to 0$, remains unchanged by the coupling to the quantum heat reservoir. This value is $T_s=J$ for when $p=2$ (Ref. 23) and it coincides with the one given by Gross and Mézard, $T_s\approx 0.67$, for the classical problem with $p=3$.[32]

For the three values of η, the static critical transverse field, $\Gamma_s(T)$, is a decreasing function of T, which is consistent with the fact that quantum fluctuations tend to destroy the glassy phase. We also see from the figures that the coupling to a quantum thermal bath favors the formation of the glassy phase: the coupling to the environment effectively reduces the strength of the quantum fluctuations that tend to destroy it. For any value of the temperature that satisfies $T<T_s^{\mathrm{class}}$ the extent of the spin-glass phase is larger for stronger couplings to the bath. Moreover, we observe that the effect of the bath is stronger for lower temperatures.

When $p=2$ the transition is always continuous and second-order thermodynamically. For $p=3$ instead, as in the spherical case[16,17,10] and the isolated quantum $S=1/2$ model,[15] an interesting change from a second-order to a first-order transition appears. We demonstrate these statements by displaying in Figs. 5 and 6 the behavior of the free-energy density, entropy, and susceptibility of the $p=3$ $S=1/2$ spin model as a function of the transverse field for $T=0.5>T_s^*$ and $T=0.3<T_s^*$.

At sufficiently high temperatures, $T\geqslant T_s^*$, one finds a spin-glass solution for increasing transverse fields until the breakpoint m reaches the value $m=1$. The values (T,Γ) where $m=1$ coincides with the ones obtained by analyzing the crossing of the free-energy densities of the paramagnetic and spin-glass solutions. Thus, for the chosen temperature $T\geqslant T_s^*$ this is the critical transverse field. Even if the Edwards-Anderson parameter, q_{ea}, and the diagonal element, $q_d(\tau)$, are nonzero at this point in parameter space, one can check, as shown in Fig. 5, that the entropy and susceptibility do not show a jump. Thus, for $T\geqslant T_s^*$ the transition is discontinuous [due to the jump in q_{ea} and $q_d(\tau)$] but of second order thermodynamically.

The situation is different at lower temperatures. In Fig. 6 we show the free energy, entropy and susceptibility of the $p=3$ $S=1/2$ model for $T=0.3<T_s^*$. In this case, the point in which the free-energy of the paramagnetic and spin-glass solution cross corresponds to $m<1$ and as shown in the figure this leads to a discontinuity of the entropy and susceptibility. In this case, the transition is discontinuous and first-order thermodynamically.

In Fig. 7 we show the dependence of q_{ea} and m on the critical temperature T_s for three values of the coupling to the bath. The model is again the $p=3$ quantum $S=1/2$ spin glass. As already mentioned we observe that for all temperatures q_{ea} is different from zero, leading to a discontinuous phase transition. m equals one for $T_s\geqslant T_s^*$ but $m<1$ for $T_s\leqslant T_s^*$. The figure also shows that T_s^* decreases with increasing coupling to the bath η. Again, this result is reminiscent of what was found in the spherical case.[10]

C. Stability of the one-step static solution

In order to study the stability of the one-step solution we evaluated the replicon eigenvalue λ_R on the values of the order parameters and m obtained from the static solution, and we searched for the parameters (T,Γ) such that λ_R vanishes. In the classical limit this yields Gardner's classical critical temperature that takes a rather low value, $T_G(\Gamma=0)\approx 0.25$.[28] Since we expect to find a decreasing value of the instability temperature with the strength of the transverse field, we need to control the numerical algorithm for $T<0.25$. Even if this might seem, at first sight, impossible, we managed to obtain sensible results keeping reachable values of M, $M\leqslant 13$, since the small values of the transverse field compensate the large value of β in the condition $\beta\Gamma/M\ll 1$.

First, we analyzed the $p=2$ case that corresponds to the SK model in a transverse field. In the absence of the environment we found that the one-step RSB solution is not stable in the full spin-glass phase supporting the idea that the solution to the statics of this model needs a full RSB scheme,

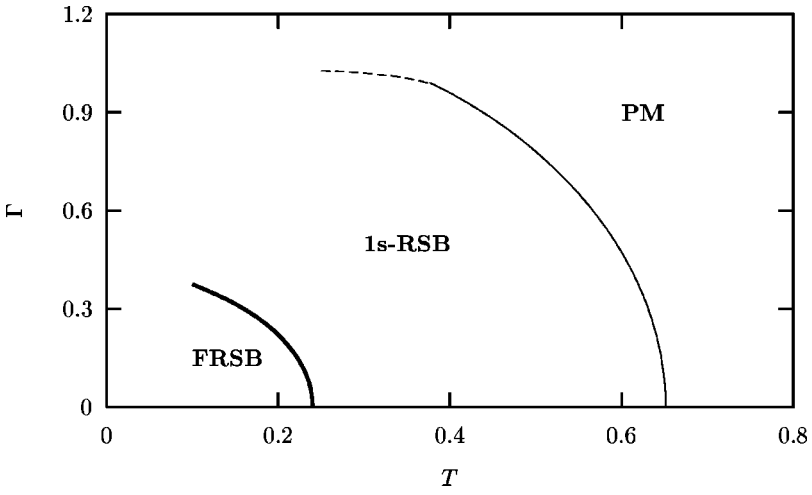

FIG. 8. Comparison between the static critical line (T_s,Γ_s) and Gardner's instability line (T_G,Γ_G) for the $p=3$ model with $\eta=0$.

just as in its classical limit and in contrast to recent claims in the literature.[33]

In Fig. 8 we compare the static critical line (T_s,Γ_s) as found from the one-step RSB *Ansatz*, with Gardner's line of instability for the $p=3$ model. We see that the region where the one-step RSB static *Ansatz* is not stable is quite small. Since we only trust the extrapolation from low values of M to $M\to\infty$ above temperatures of the order of $T\approx 0.1$, we do not explicitly extrapolate the instability line to lower temperatures. Nevertheless, the existing data suggest that in the zero temperature limit the static critical transverse field, Γ_s, and Gardner's critical field, Γ_G, do not coincide $\Gamma_s(T_s=0)>\Gamma_G(T_G=0)$.

D. The dynamic transition

As already explained in Sect. II the value of m found by setting the replicon eigenvalue to zero leads to different equations that encode some information about the nonequilibrium relaxation dynamics of the system. Using this prescription we obtained, for the $p\geqslant 3$ models a different critical line that lies above the static transition. This result is similar to those found in a series of other classical[25] and quantum[15–17] problems. In Fig. 9 we compare the static and marginal critical lines for the $p=10$ quantum $S=1/2$ model. We chose a larger value of p to make the difference between the two lines easier to visualize. The glassy static region is smaller than the glassy region determined by the marginality condition. When approaching the glassy phase from any direction in parameter space, the dynamic transition, associated to the line of marginal stability, occurs before the static one. As on the critical static line, the curve determined with the marginal stability criterion is made of two pieces, on one of them the transition is of second-order (indicated with a solid line in Fig. 9) and on the other the transition is of first-order (indicated with a dashed line on the same figure). The first-order nature of the dynamic transition is displayed by, for instance, a jump in the asymptotic value of the averaged internal energy. The marginal tricritical point occurs at higher temperature than the static one.

The external noise also has a strong effect on the dynamic critical line. The stronger the coupling to the environment (larger value of η), the larger the spin-glass region in the phase diagram. This is also shown in Fig. 9 where a couple of curves, corresponding to $\eta=0$ and $\eta=0.5$ are drawn (see the caption in the figure for more details).

Finally, let us mention that there is an empirical relation between the value of the parameter m as found from the marginality condition and how the fluctuation-dissipation theorem is modified in the real time nonequilibrium relax-

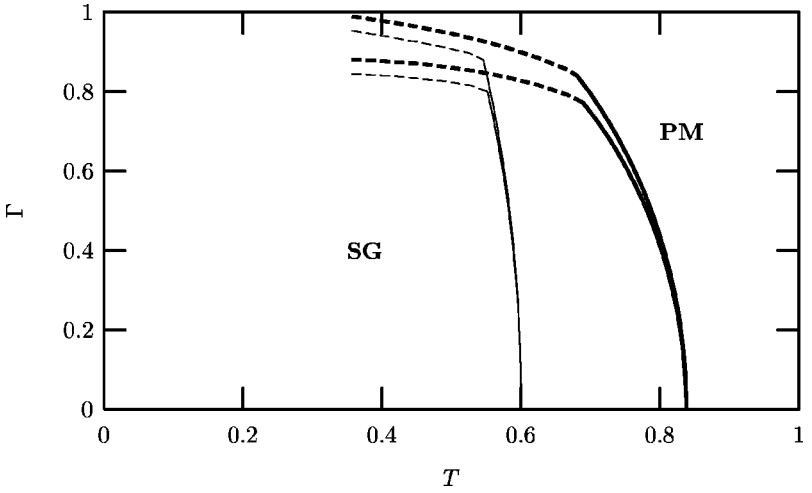

FIG. 9. Comparison between the static and marginal critical lines for the $p=10$ model. The solid lines represent second order transitions and the dashed lines first order ones. The set of curves with $T_s^{\rm class}\approx 0.6$ (thin lines) are the static transition lines for $\eta=0$ (below) and $\eta=1$ (above); the set of curves with $T_s^{\rm class}\approx 0.82$ (bold lines) correspond to the dynamic transition for $\eta=0$ (below) and $\eta=1$ (above).

ation of the quantum model.[9,10] Using this relation and interpreting then the parameter m/T as an effective temperature[34] we find that the modification of the fluctuation-dissipation theorem, and hence, $T_{\rm eff}$, depend on the strength of the coupling to the bath.

IV. CONCLUSIONS

In this paper we studied the effect of an Ohmic quantum bath on the statics and dynamics of quantum disordered $S=1/2$ spin models of mean-field type. We found that the coupling to the environment favors the appearance of the spin-glass phase reducing the strength of the quantum fluctuations that tend to destabilize it. As in the case of the spherical model[10,11] the phase transition is always second order for $p=2$. For $p\geqslant 3$ there exists a tricritical temperature $T^\star$ below which quantum fluctuations drive the transition first order. $T^\star$ decreases with the strength of the coupling to the bath. For $p\geqslant 3$ a dynamic transition precedes the equilibrium phase transition. The coupling to the bath also stabilizes the dynamic glassy phase.

The physical origin of these effects is very simple: friction and spin-spin interactions separately counteract the transverse field tending to suppress quantum fluctuations. When the two effects are simultaneously present they reinforce each other.

It would be interesting to check if the same tendency to ordering appears in macroscopic spin models in finite dimensions. One could attempt to study this problem in the context of frustrated spin magnets or the much studied, numerically and analytically, quantum $S=1/2$ spin chain with and without disorder. This problem is of interest for the possible implementation of quantum computers where the interaction of the system with its environment needs to be controlled. The effect of an environment on the properties of Griffith phases has also been the focus of a hot debate.[35] We expect to report on these problems in the near future.

ACKNOWLEDGMENTS

The authors acknowledge financial support from the Ecos-Sud travel grant, the ACI project "Optimisation algorithms and quantum disordered systems." L.F.C. is research associate at ICTP Trieste and acknowledges financial support from the J. S. Guggenheim Foundation. G.S.L. was supported by EPSRC Grants Nos. GR/N19359 and GR/R70309. This research was supported in part by the National Science Foundation under Grant No. PHYS99-07949. G.L. acknowledges financial support from CONICET under PICT 03–11609. The authors thank F. Ritort for very useful discussions.

[1] A. J. Leggett, S. Chakravarty, A. T. Dorsey, M. P. A. Fisher, A. Garg, and W. Zwerger, Rev. Mod. Phys. **59**, 1 (1987); **67**, 725 (1995).

[2] U. Weiss, *Series Modern Condensed Matter Physics* (World Scientific, Singapore, 1993), Vol. 2.

[3] W. Wu, B. Ellman, T. F. Rosenbaum, G. Aeppli, and D. H. Reich, Phys. Rev. Lett. **67**, 2076 (1991); W. Wu, D. Bitko, T. F. Rosenbaum, and G. Aeppli, Appl. Phys. Lett. **71**, 1919 (1993).

[4] R. Vollmer, T. Pietrus, H. v. Löhneysen, R. Chau, and M. B. Maple, Phys. Rev. B **61**, 1218 (2000).

[5] Y. Tabata, D. R. Grempel, M. Ocio, T. Taniguchi, and Y. Miyako, Phys. Rev. Lett. **86**, 524 (2001).

[6] F. Ladieu, J. Le Cochec, P. Pari, P. Trouslard, and P. Ailloud, Phys. Rev. Lett. **90**, 205501 (2003); S. Ludwig and D. D. Osheroff, *ibid.* **91**, 105501 (2003); S. Rogge, D. Natelson, and D. D. Osheroff, *ibid.* **76**, 3136 (1996).

[7] D. R. Grempel and M. J. Rozenberg, Phys. Rev. Lett. **80**, 389 (1998); M. J. Rozenberg and D. R. Grempel, *ibid.* **81**, 2550 (1998).

[8] H. Rieger and A. P. Young, *Quantum Spin Glasses* (Springer-Verlag, Berlin, 1996); cond-mat/9607005 (unpublished); R. Bhatt, in *Spin-Glasses and Random Fields*, edited by A. P. Young (World Scientific, Singapore, 1997).

[9] L. F. Cugliandolo and G. Lozano, Phys. Rev. Lett. **80**, 4979 (1998); Phys. Rev. B **59**, 915 (1999).

[10] L. F. Cugliandolo, D. R. Grempel, G. Lozano, H. Lozza, and C. A. da Silva Santos, Phys. Rev. B **66**, 014444 (2002).

[11] M. Rokhni and P. Chandra, Phys. Rev. B **69**, 094403 (2004).

[12] G. Biroli and O. Parcollet, Phys. Rev. B **65**, 094414 (2002).

[13] N. Pottier and A. Mauger, Physica A **282**, 77 (2000).

[14] D. R. Grempel and M. J. Rozenberg, Phys. Rev. B **60**, 4702 (1999).

[15] T. M. Nieuewenhuizen and F. Ritort, Physica A **250**, 89 (1998).

[16] L. F. Cugliandolo, D. R. Grempel, and C. A. da Silva Santos, Phys. Rev. Lett. **85**, 2589 (2000).

[17] L. F. Cugliandolo, D. R. Grempel, and C. A. da Silva Santos, Phys. Rev. B **64**, 014403 (2001).

[18] G. Biroli and L. F. Cugliandolo, Phys. Rev. B **64**, 014206 (2001).

[19] Y. Y. Goldschmidt and P.-Y. Lai, Phys. Rev. Lett. **64**, 2467 (1990); P.-Y. Lai and Y. Y. Goldschmidt, Europhys. Lett. **13**, 289 (1990).

[20] R. P. Feynman and F. L. Vernon, Jr., Ann. Phys. (N.Y.) **24**, 118 (1963); R. P. Feynman, *Statistical Mechanics* (Addison-Wesley, Reading, MA, 1972).

[21] A. Caldeira and A. Leggett, Phys. Rev. Lett. **46**, 211 (1981); A. Caldeira and A. Leggett, Ann. Phys. (N.Y.) **149**, 374 (1983).

[22] D. R. Grempel and M. J. Rozenberg, Phys. Rev. B **60**, 4702 (1999).

[23] M. Mézard, G. Parisi, and M. A. Virasoro, *Spin Glass Theory and Beyond* (World Scientific, Singapore, 1987).

[24] A. J. Bray and M. A. Moore, J. Phys. C **13**, L655 (1980).

[25] T. R. Kirkpatrick and D. Thirumalai, Phys. Rev. B **36**, 5388 (1987); T. R. Kirkpatrick and P. G. Wolynes, *ibid.* **36**, 8552 (1987); L. F. Cugliandolo and J. Kurchan, Phys. Rev. Lett. **71**, 173 (1993).

[26] T. Giamarchi and P. Le Doussal, Phys. Rev. B **53**, 15206 (1996); A. Georges, O. Parcollet, and S. Sachdev, Phys. Rev. Lett. **85**, 840 (2000); Phys. Rev. B **63**, 134406 (2001); G. Schehr, T.

Giamarchi, and P. Le Doussal, cond-mat/0212300 (unpublished).
[27] J. R. L. de Almeida and D. J. Thouless, J. Phys. A **11**, 983 (1978).
[28] E. Gardner, Nucl. Phys. B **257** [FS14], 747 (1985).
[29] K. D. Usadel and B. Schmitz, Solid State Commun. **64**, 975 (1987).
[30] J. V. Alvarez and F. Ritort, J. Phys. A **29**, 7355 (1996).
[31] M. Suzuki, Prog. Theor. Phys. **56**, 1454 (1976).
[32] D. J. Gross and M. Mézard, Nucl. Phys. B **240**, [FS12] 431 (1984).
[33] D.-H. Kim and J.-J. Kim, Phys. Rev. B **66**, 054432 (2002).
[34] L. F. Cugliandolo, J. Kurchan, and L. Peliti, Phys. Rev. E **55**, 3898 (1997).
[35] A. H. Castro-Neto and B. A. Jones, Phys. Rev. B **62**, 14975 (2000); A. J. Millis, D. Morr, and J. Schmalian, *ibid.* **66**, 174433 (2002).